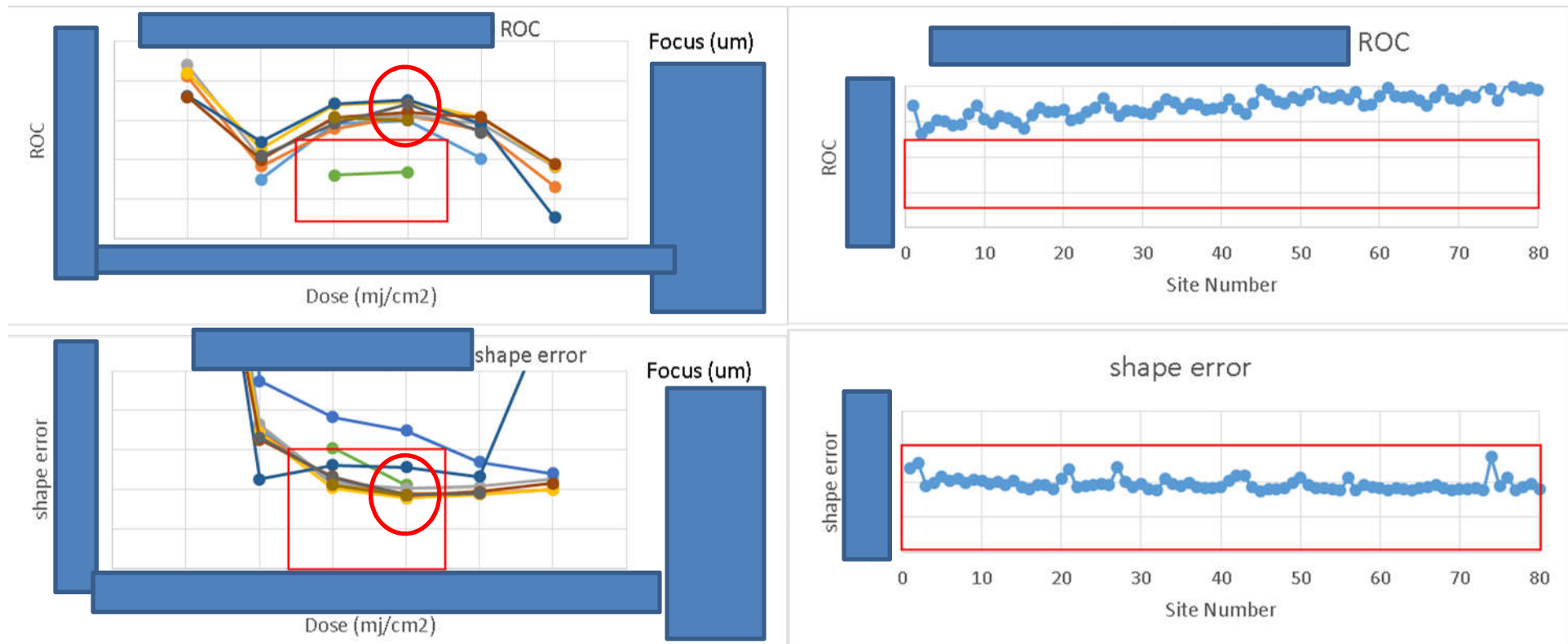
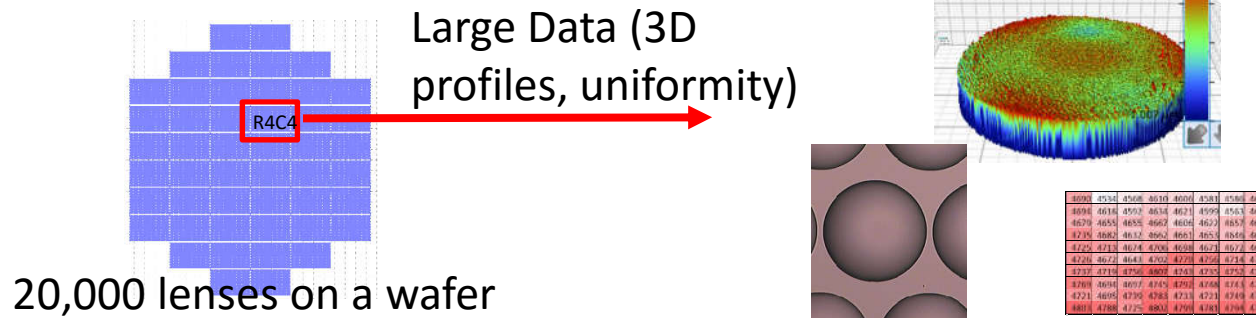
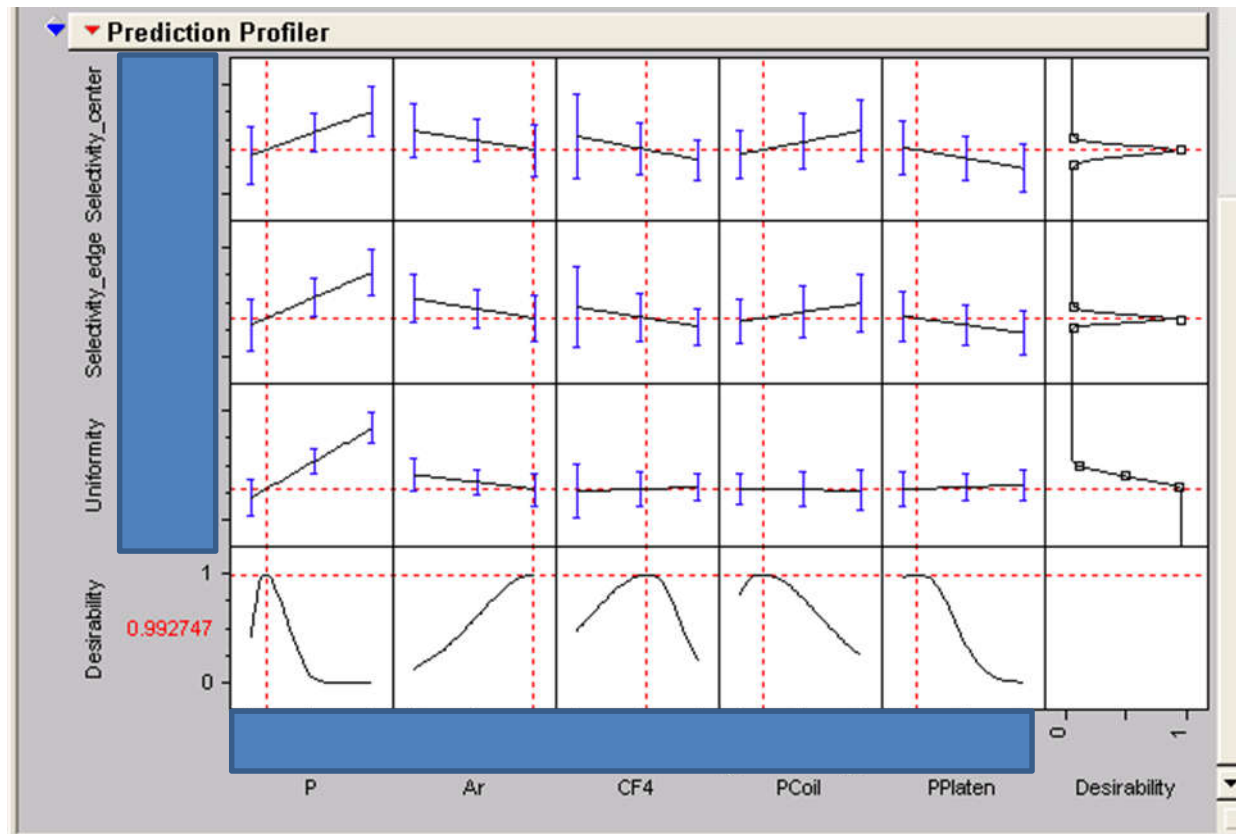


# Microlens Array (IMT, 2013-present)



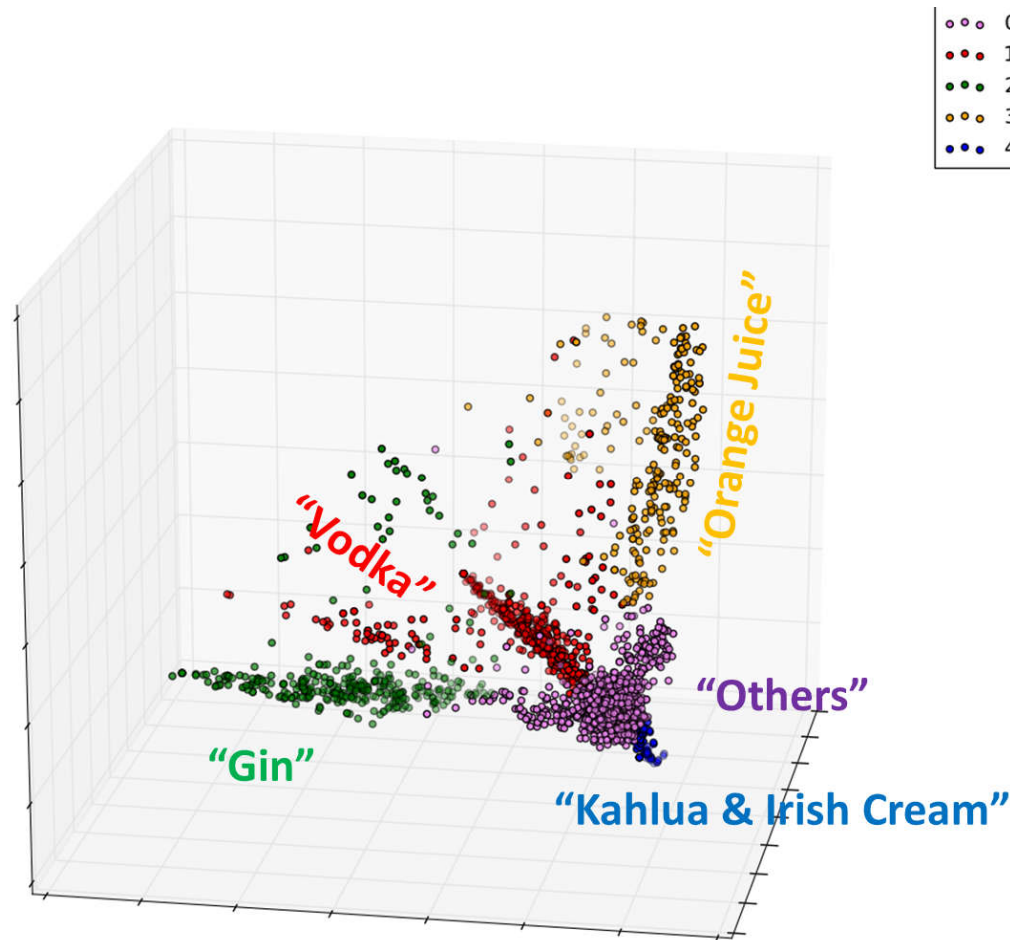
- Processed data essential for the success of this project.
- Transitioning to a volume production phase

# JMP (IMT, 2013-present)



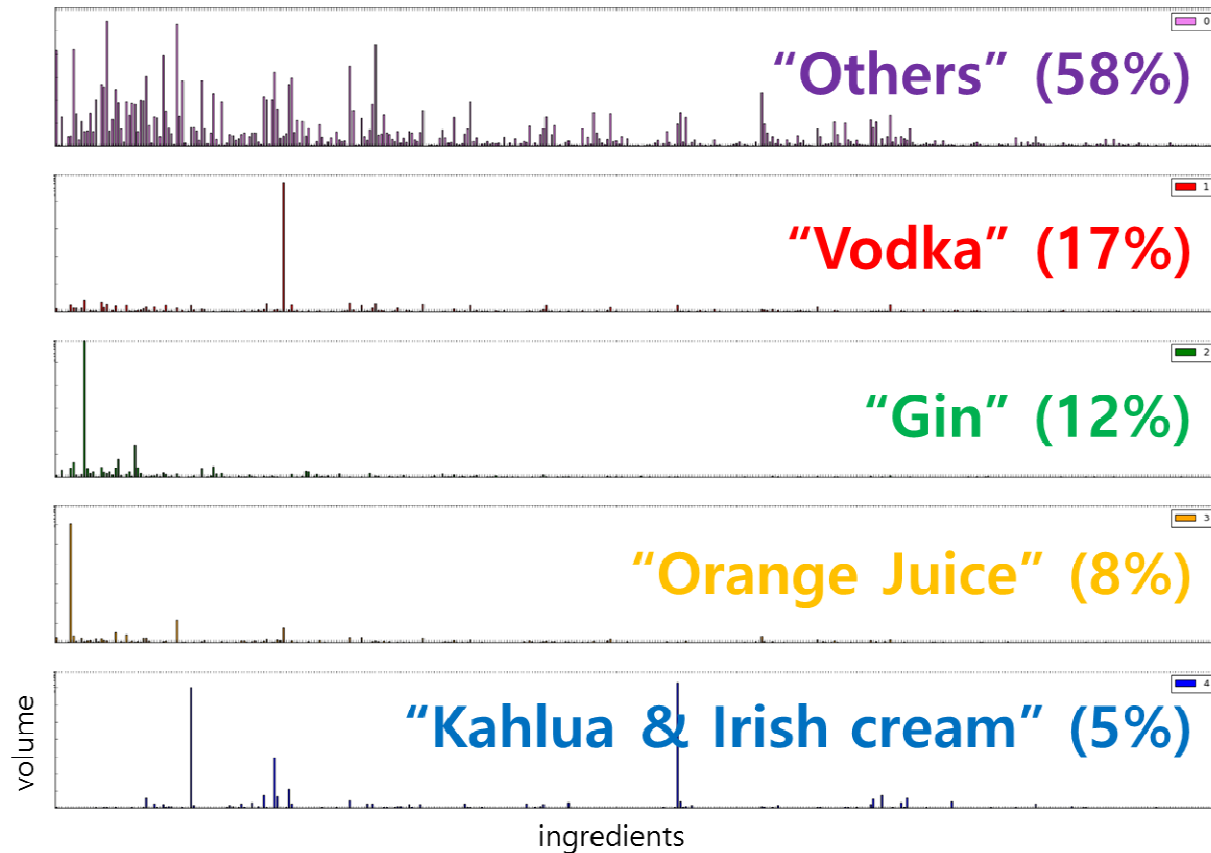
- SAS JMP used for optimizing process

# Python programming as a hobby (2016)



- 3081 cocktail recipes were downloaded from <http://www.TheCocktailDB.com> using their API.
- Each cocktail was embedded in a 471-dimensional vector space using ingredient information.
- Principal Component Analysis (PCA) was used in order to visualize 3081 cocktails in a 3D space.
- Spectral Cluster algorithm was used to separate the groups
- Generated profiles of each market segment.

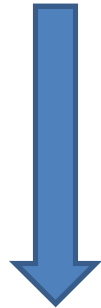
# Python programming as a hobby (2016)



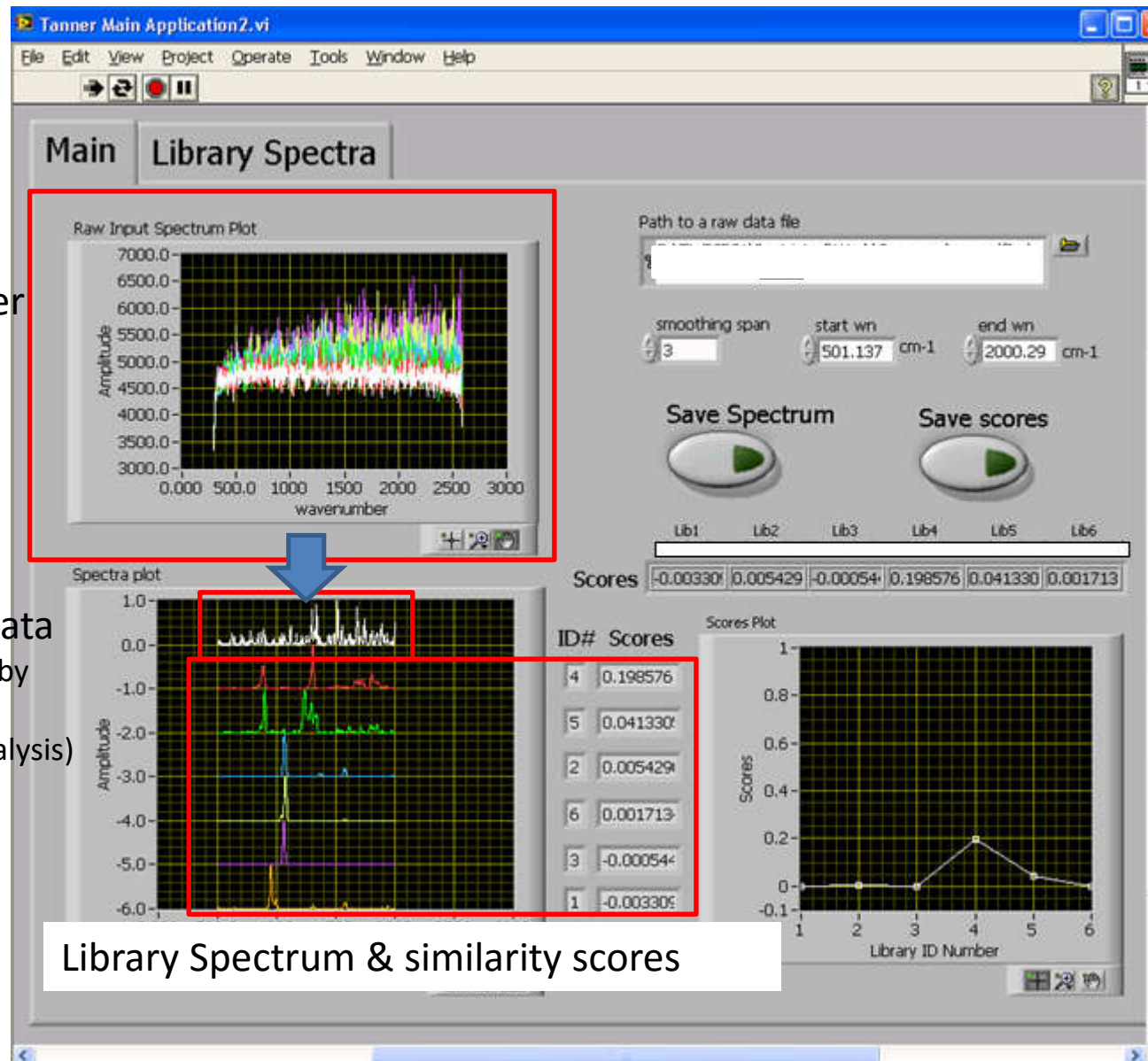
- Cocktail Recipes were downloaded from <http://www.TheCocktailDB.com> using their API.
- Each cocktail was embedded in 471-dimensional vector space using ingredient information.
- Principal Component Analysis (PCA) was used in order to visualize 3081 cocktails in a 3D space.
- Spectral Cluster algorithm was used to separate the groups
- Generated profiles of each market segment.

# Chemical Detection (Tanner Research, 2009-2013)

Raw Data  
from  
spectrometer



Processed Data  
(noise reduced by  
Principal  
Component Analysis)



Library Spectrum & similarity scores

# Chemical Detection (Tanner Research, 2009-2013)

Name	Formula for Scores (worst=0, best=1)
Euclidean Distance (ED)	$S_k = \frac{L_k \cdot U}{\sqrt{L_k \cdot L_k} \sqrt{U \cdot U}} (= \cos \theta_k, \text{ where } \theta_k \text{ is the angle between } L_k \text{ and } U)$
Correlation (CO)	$S_k = \frac{L_k' \cdot U'}{\sqrt{L_k' \cdot L_k'} \sqrt{U' \cdot U'}}, \text{ where } L_k' = L_k - \frac{\sum_{i=1}^n L_{ki}}{n} \text{ and } U' = U - \frac{\sum_{i=1}^n U_i}{n}$
Absolute Value (AV)	$S_k = 1 - \frac{\sum_{i=1}^n  L_{ki} - U_i }{n}$
Least Squares (LS)	$S_k = 1 - \frac{\sum_{i=1}^n (L_{ki} - U_i)^2}{n}$
Single Chemical Library Regression (PCR)	$S = UL^t(LL^t)^{-1}, \text{ assuming } U = SL \text{ holds true.}$

$n$ : number of spectral data points (e.g., 1024)

$U$ : unknown spectrum vector (e.g., 1x1024)

$L$ : library spectra matrix (e.g., 6x1024)

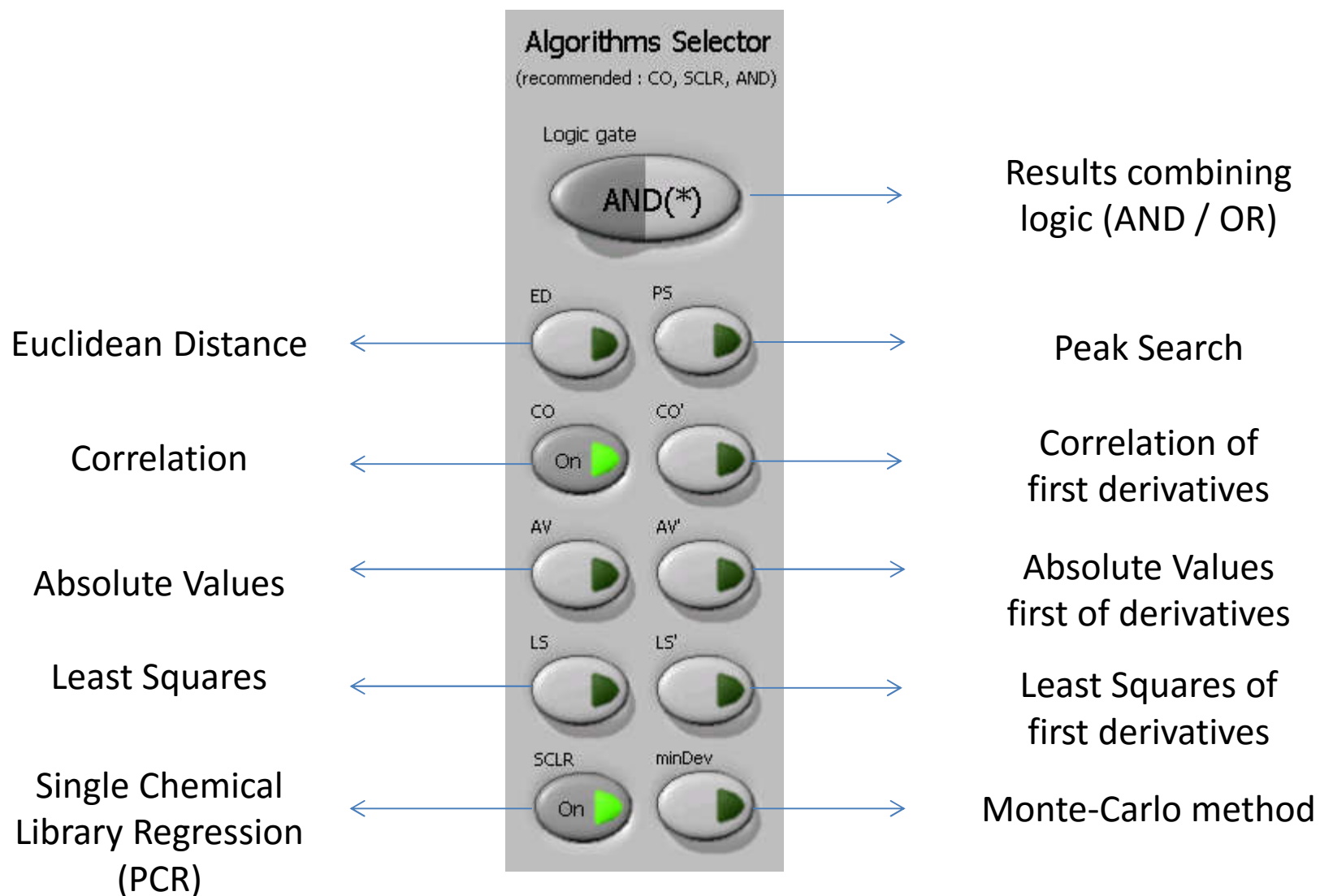
$S$ : score matrix (e.g., 1x6)

$L_k$ : k-th library spectrum vector (e.g., 1x1024)

$L_{ki}$ : i-th spectral component of k-th library spectrum vector

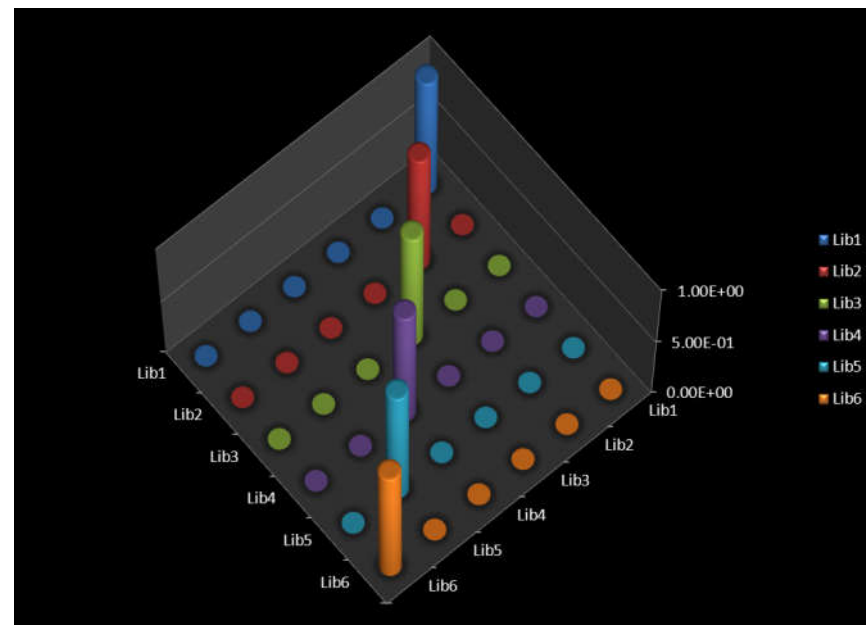
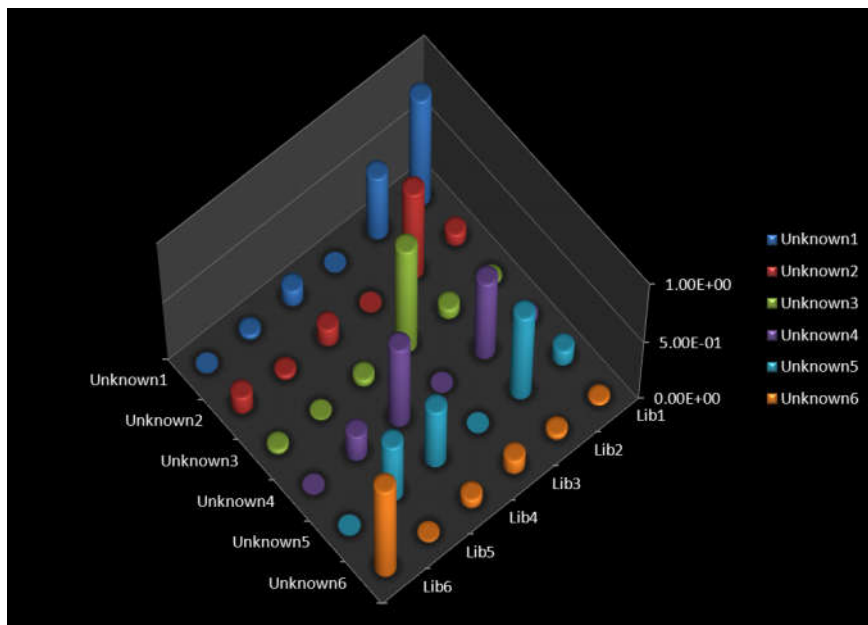
$S_k$ : score of unknown vector against k-th library spectrum vector

# Chemical Detection (Tanner Research, 2009-2013)





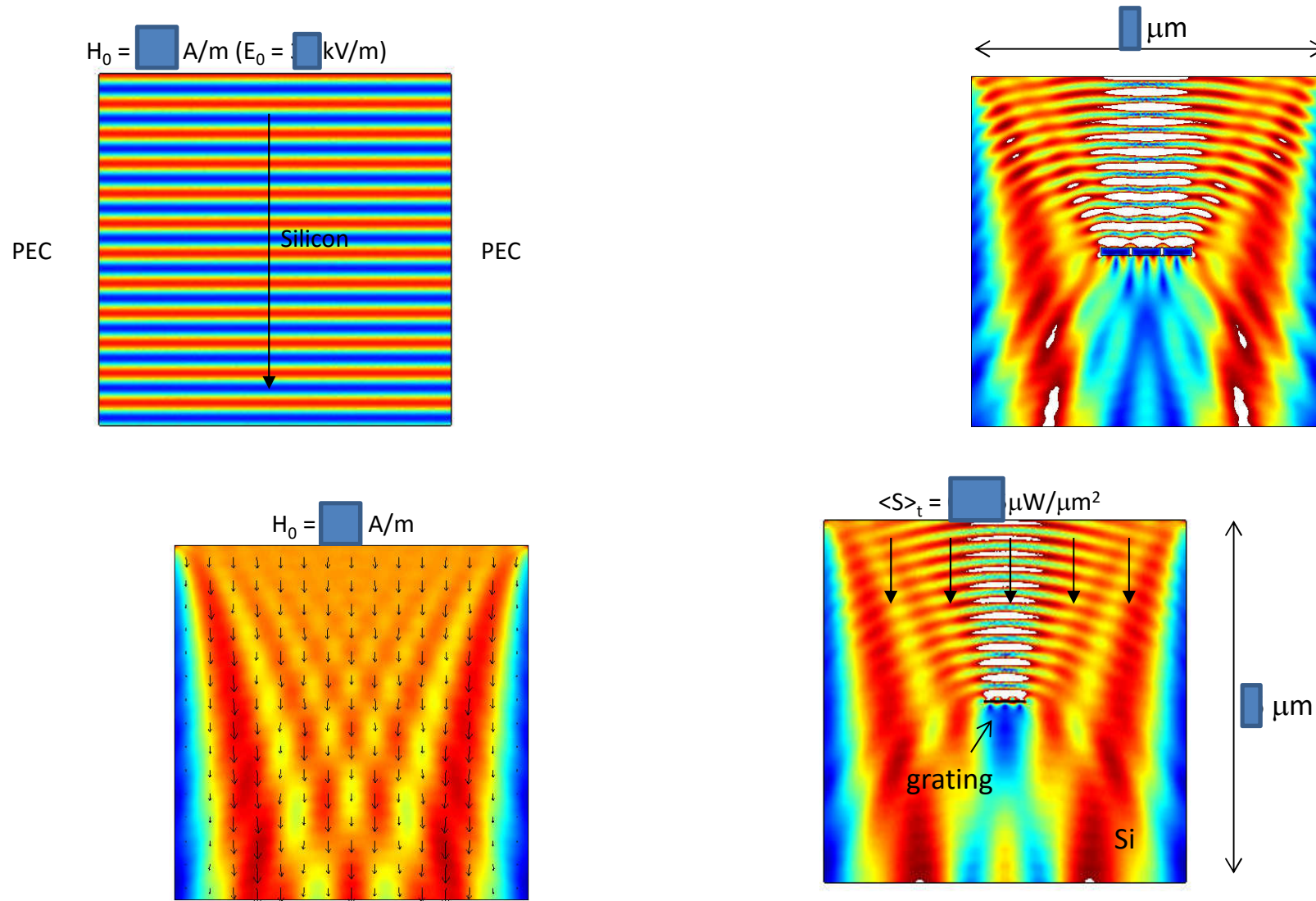
# *Chemical Detection Algorithms*



- This standoff-chemical detection system passed rigorous field tests (accuracy, recall) at customer's proving ground. Customer later asked us to deliver software only.



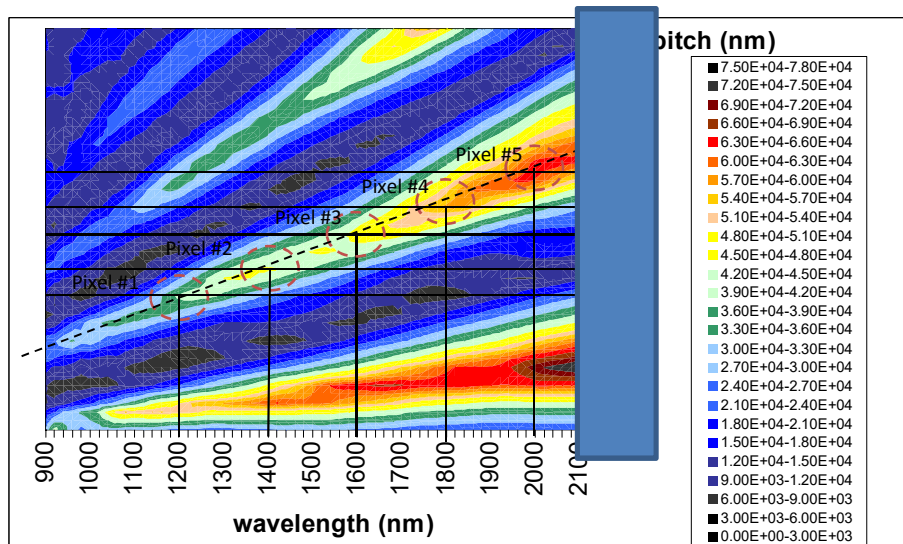
# Multispectral Infrared Metamaterial (Tanner Research, 2009-2013)



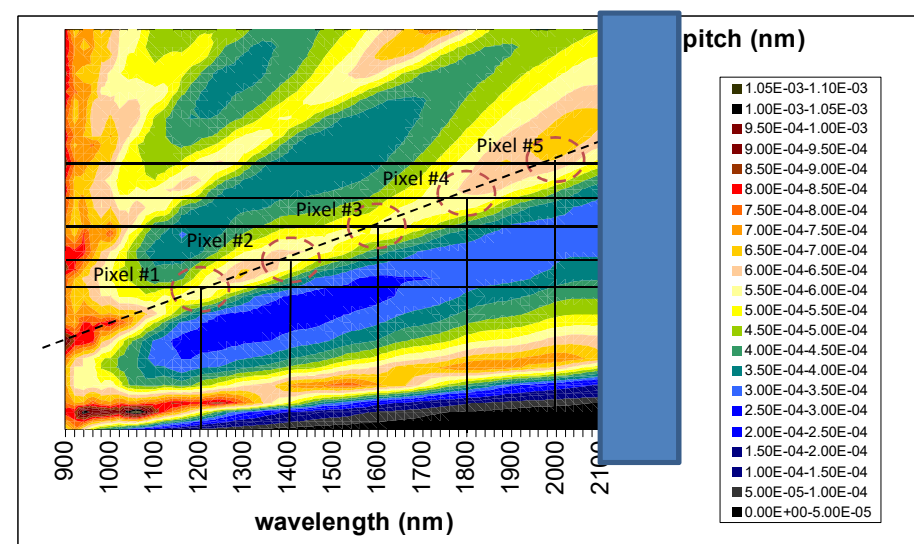
# Multispectral Infrared Metamaterial (Tanner Research, 2009-2013)

Strong E-fields and large  $\Delta T$  when pitch =  $(2n-1)/2 * \lambda_{spp}$ ,  $n = 1, 2, 3, \dots$   
 Weak E-fields and small  $\Delta T$  when pitch =  $n * \lambda_{spp}$ ,  $n = 1, 2, 3, \dots$   
 Reference: D. Pacifici, *et al.*, PRB 77, 115411 (2008)

E-fields

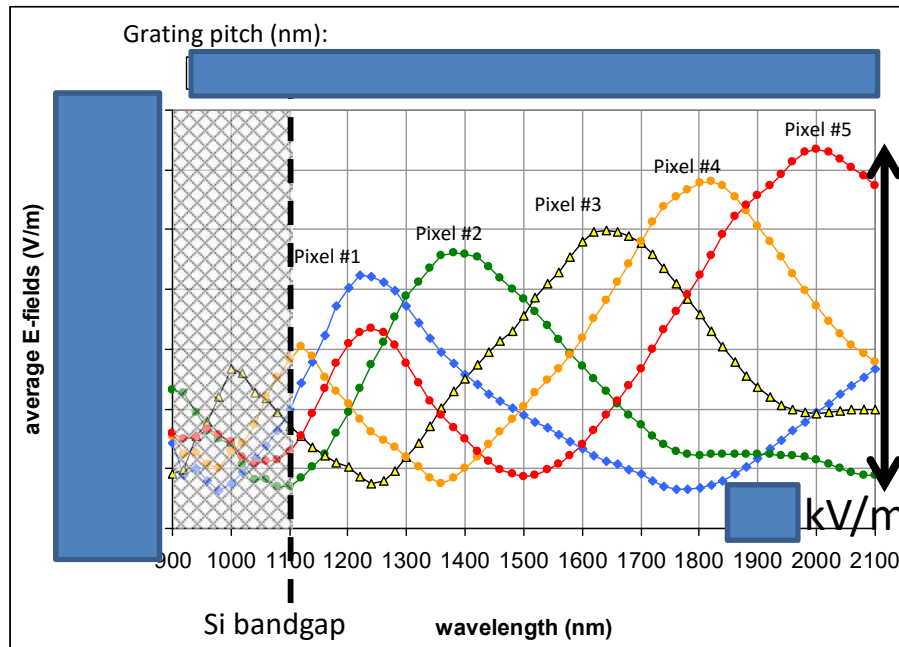


$\Delta T$

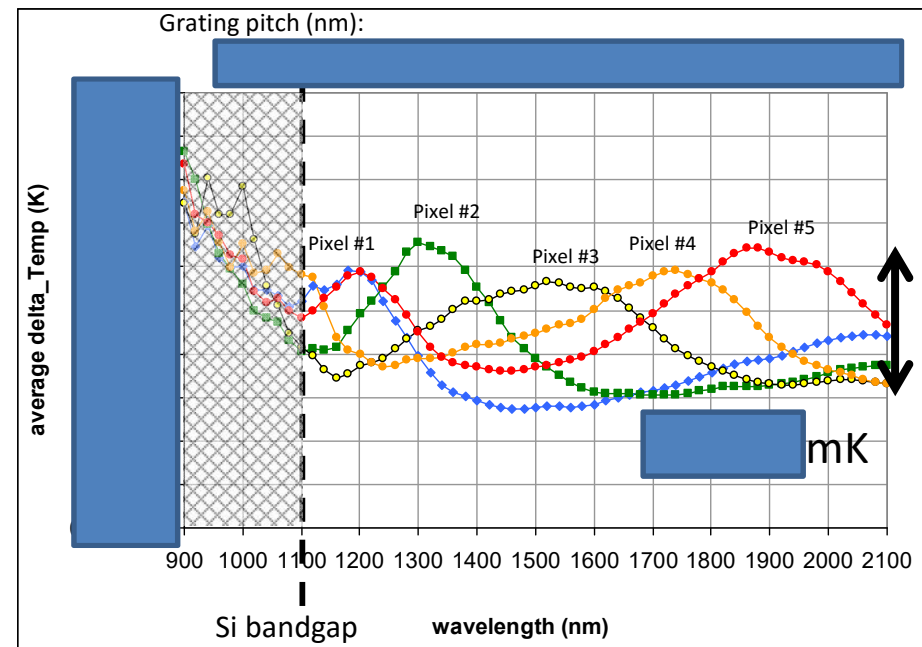


# Multispectral Infrared Metamaterial (Tanner Research, 2009-2013)

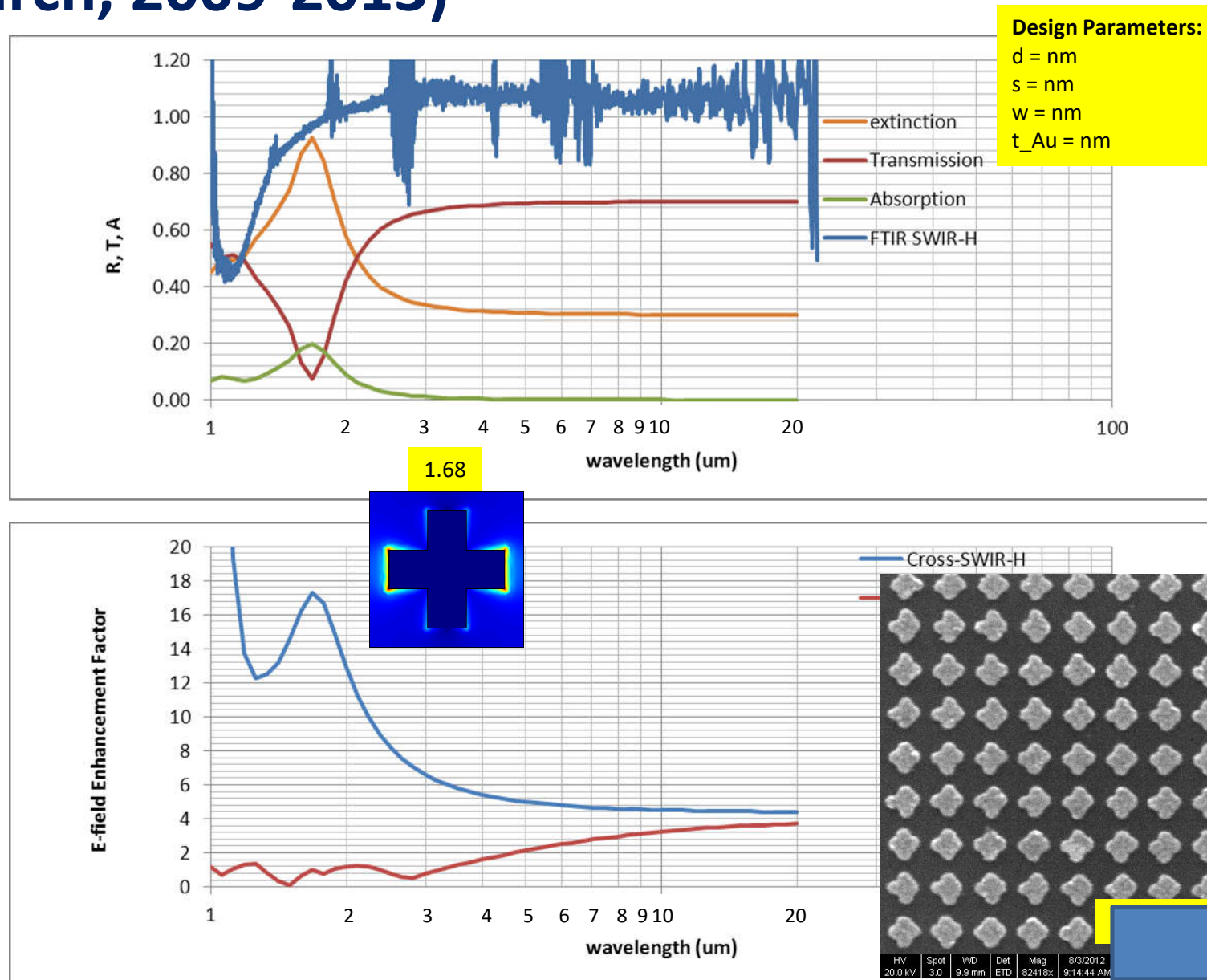
Average E-fields on the gaps



average  $\Delta T$  (temperature change due to ohmic heating) on the gaps

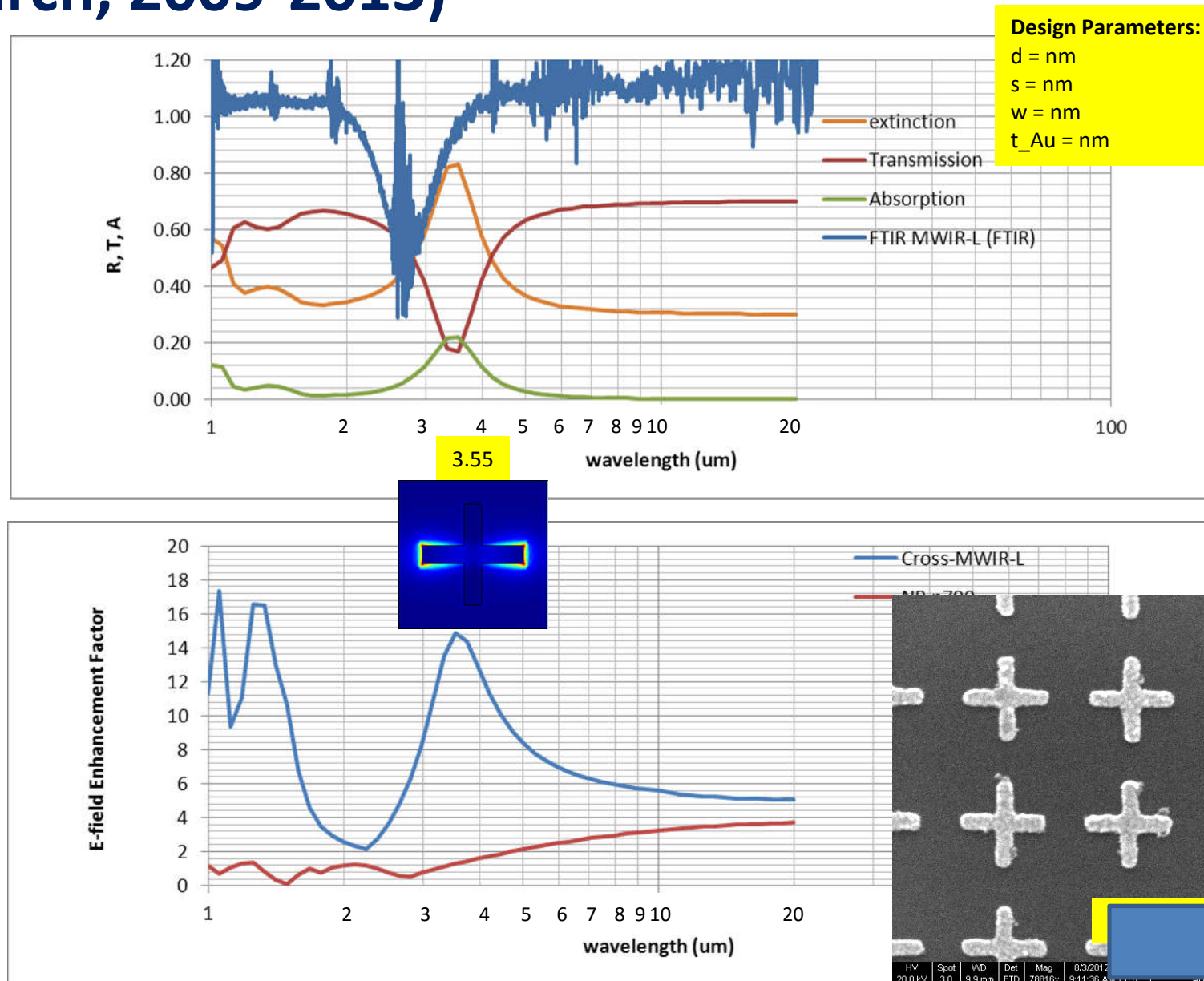


# Multispectral Infrared Metamaterial (Tanner Research, 2009-2013)

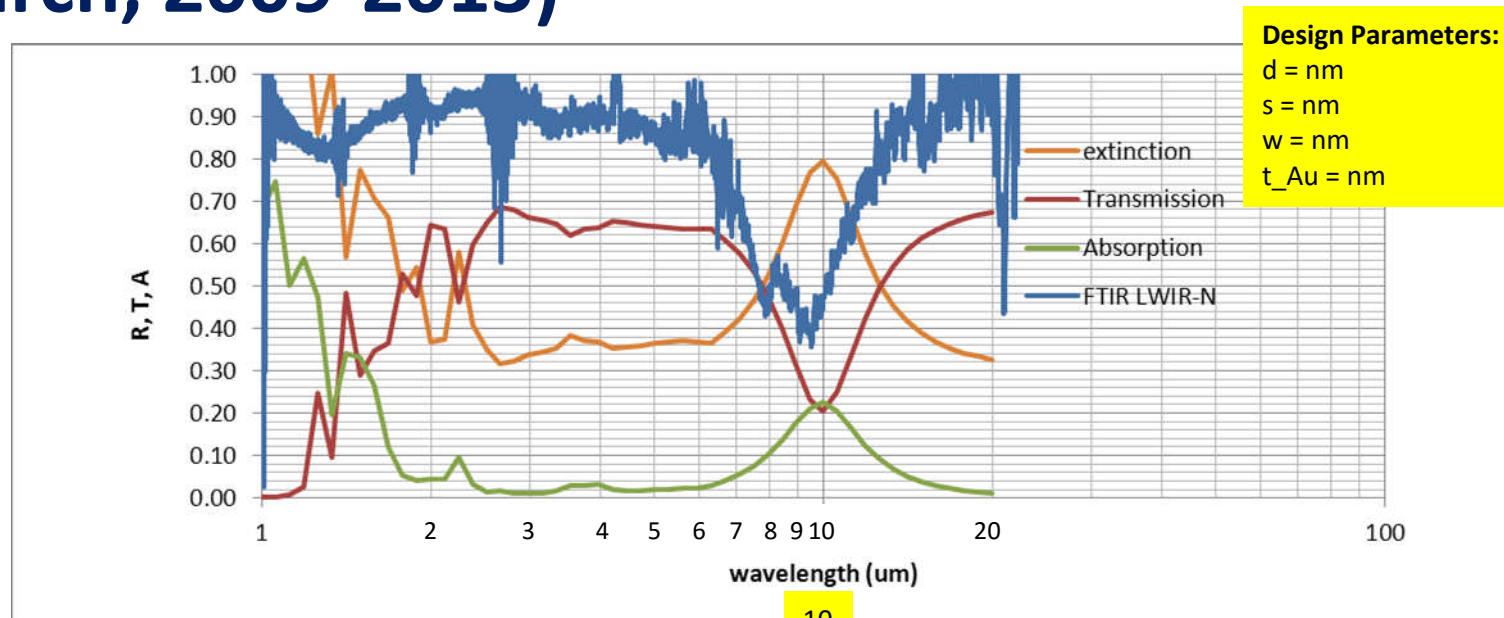




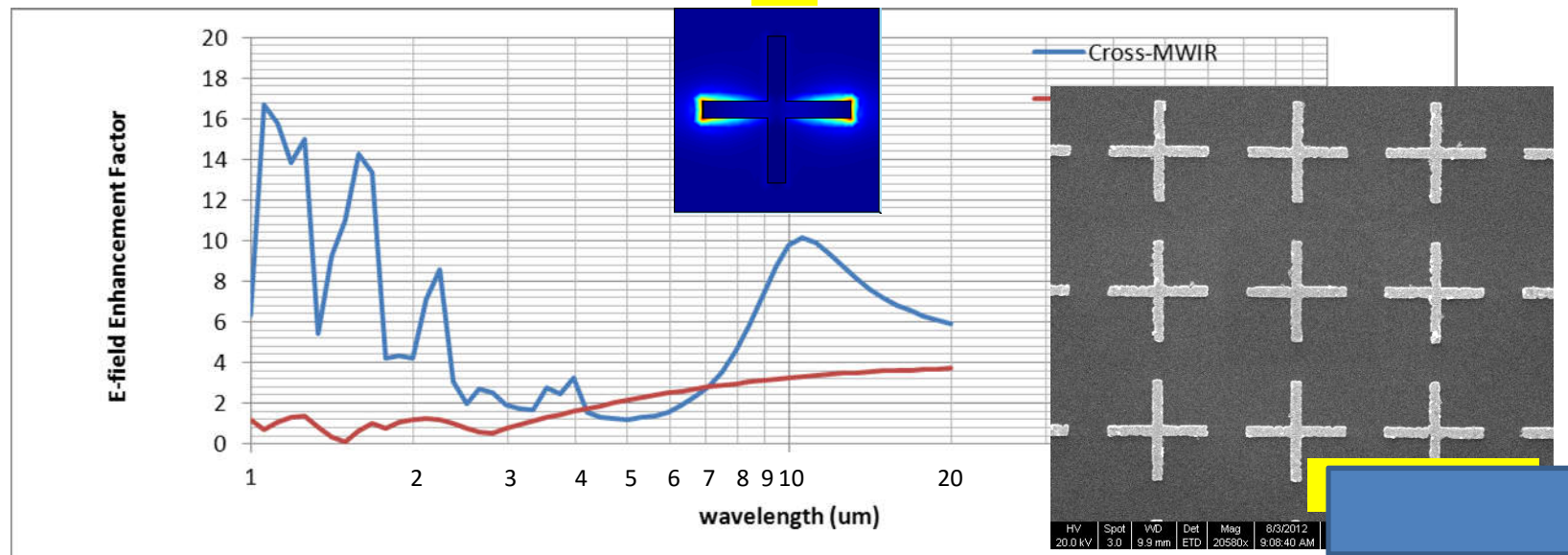
# Multispectral Infrared Metamaterial (Tanner Research, 2009-2013)



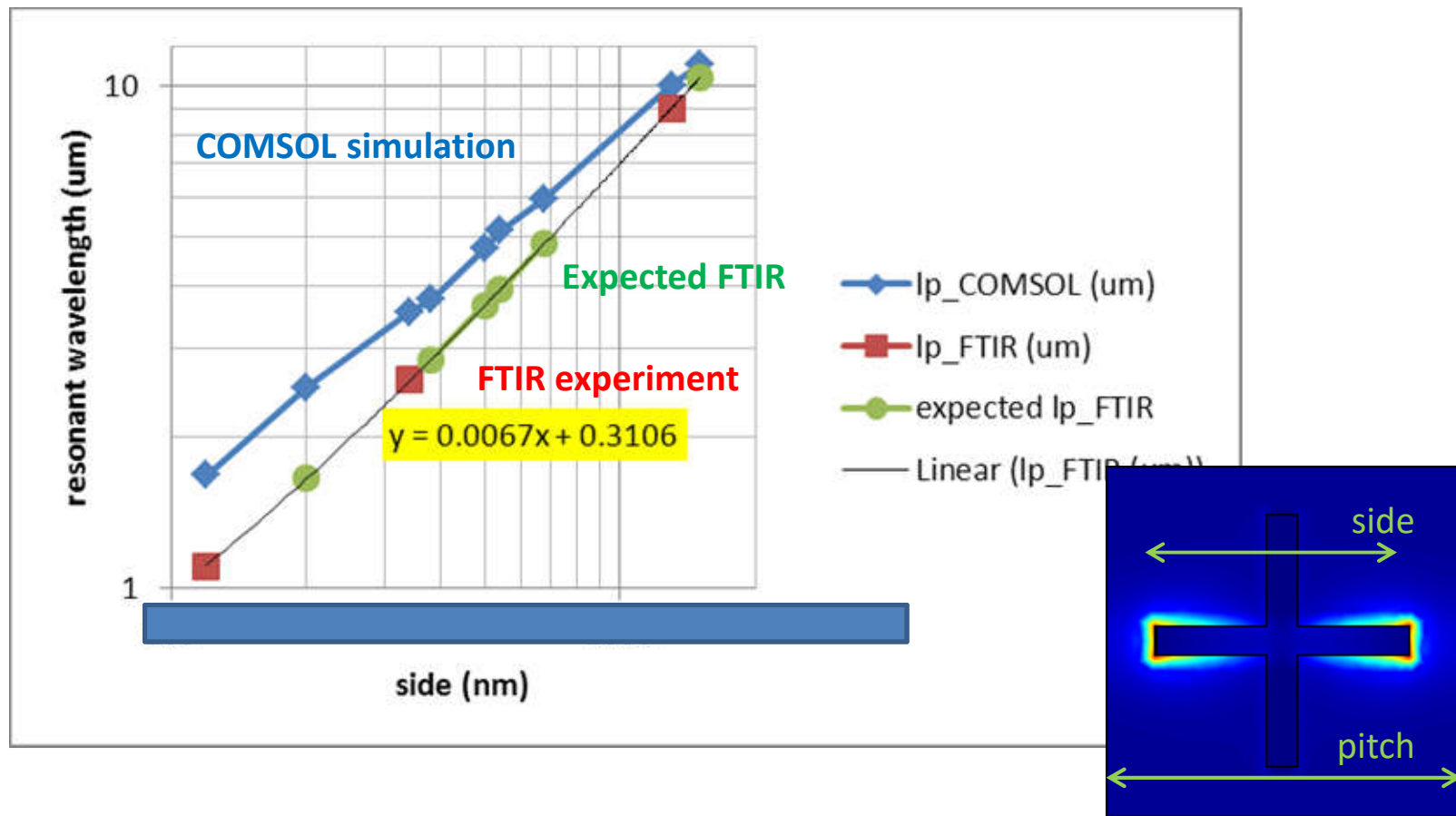
# Multispectral Infrared Metamaterial (Tanner Research, 2009-2013)



10



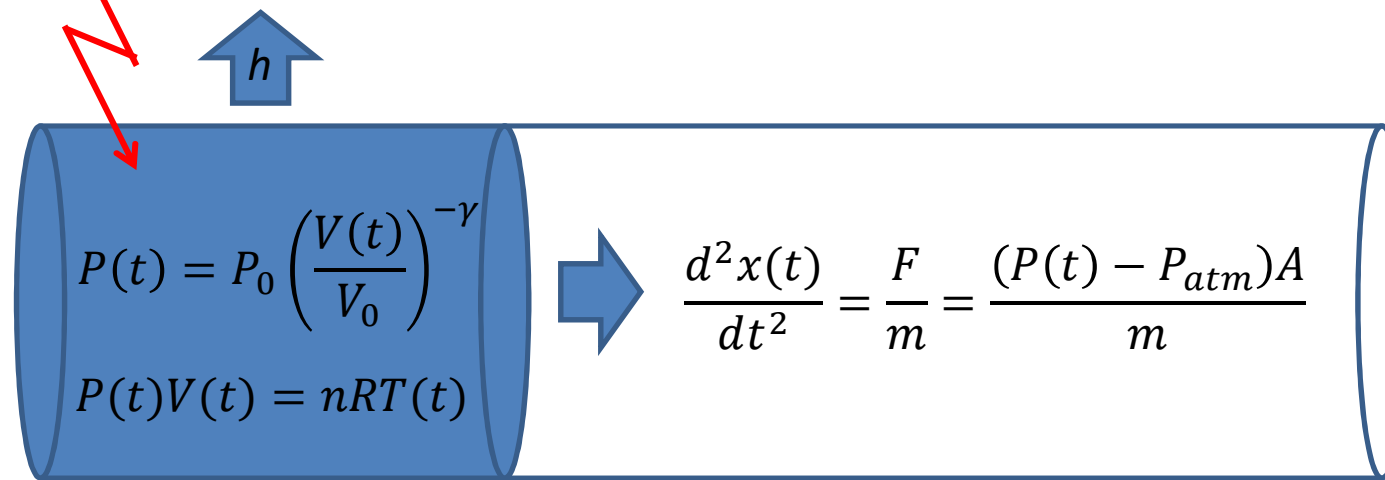
# Multispectral Infrared Metamaterial (Tanner Research, 2009-2013)





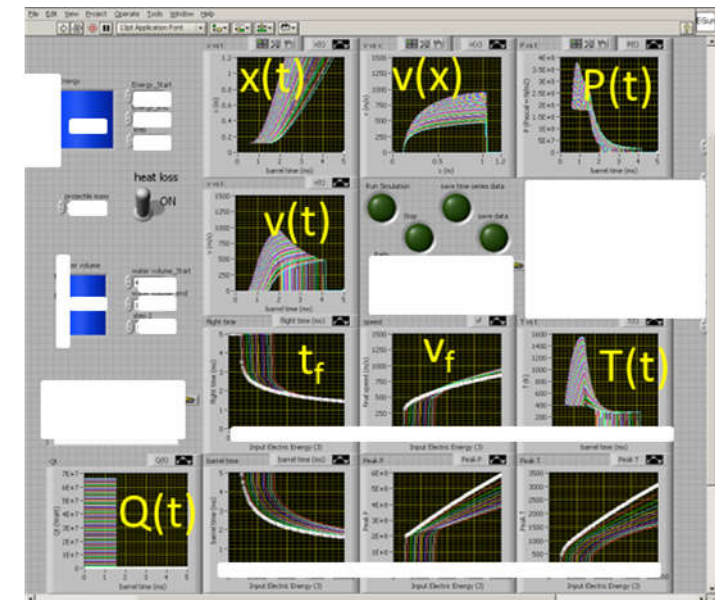
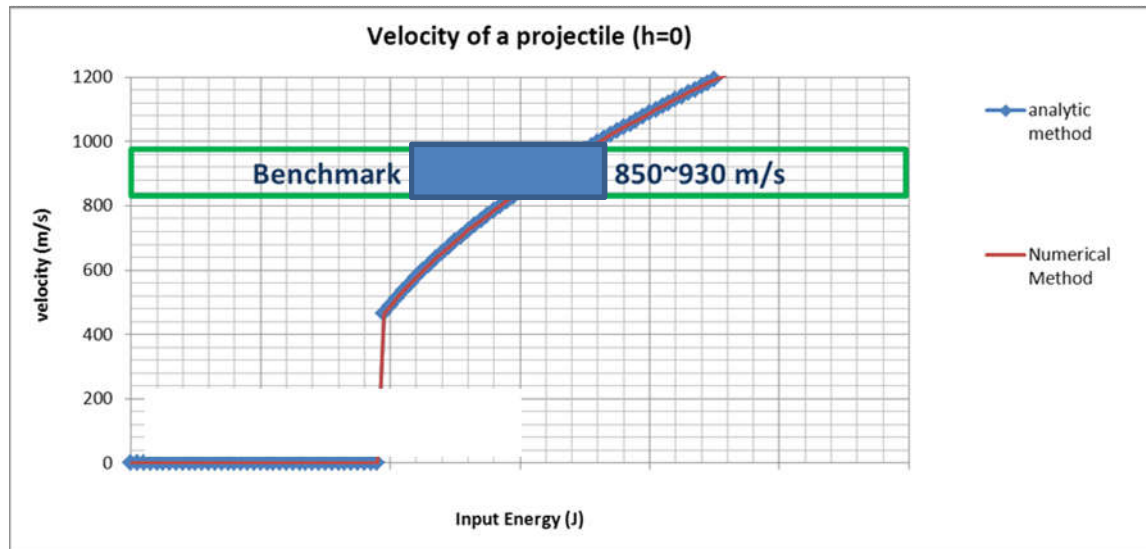
# Numerical Methods Simulation (Tanner Research, 2009-2013)

$$MC_V \frac{dT(t)}{dt} = Q(t) - h \cdot (2\pi r) \cdot x(t) \cdot (T(t) - T_{barrel})$$

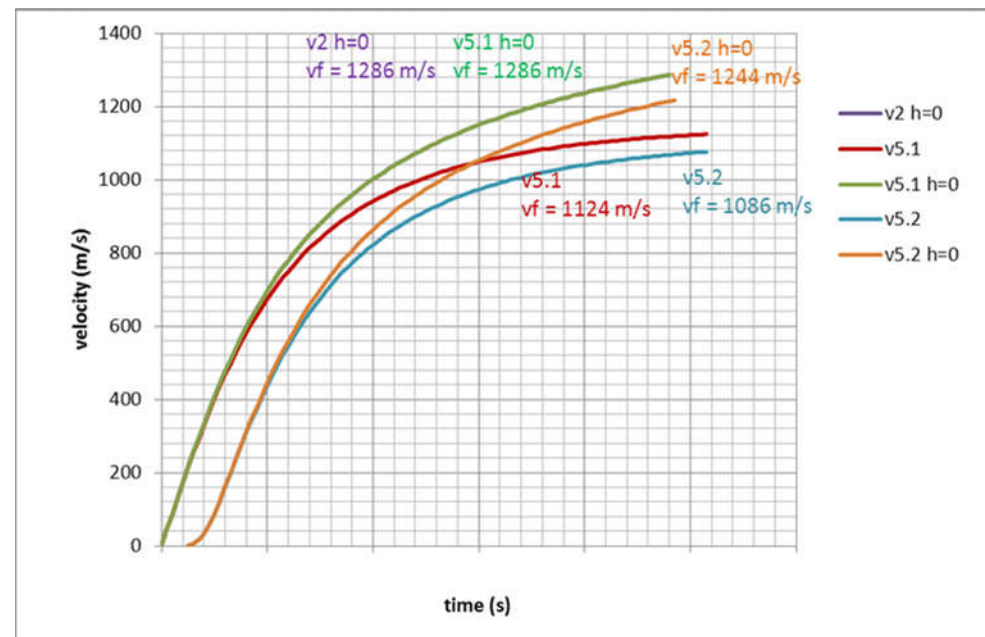
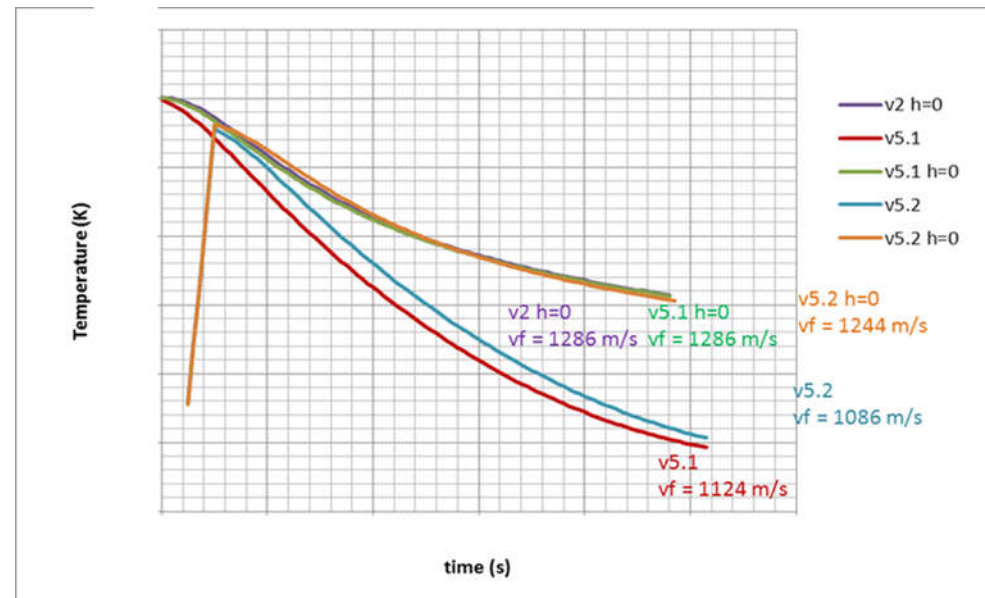


$$v_f = ?$$

$$t_f = ?$$

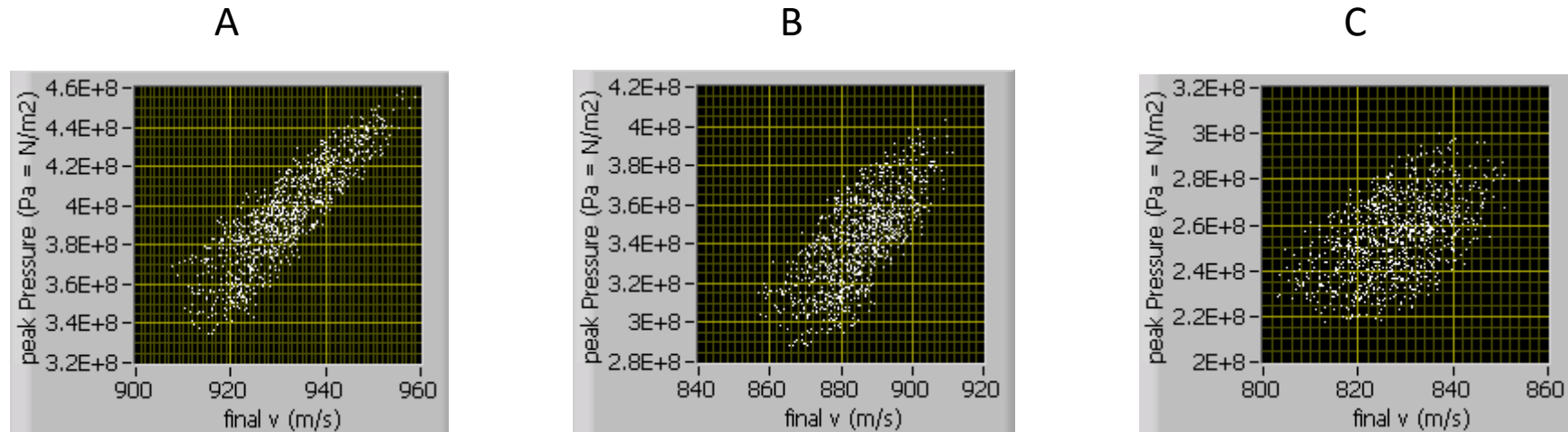


# Numerical Methods Simulation (Tanner Research, 2009-2013)



# Numerical Methods Simulation (Tanner Research, 2009-2013)

## Monte-Carlo Method (optimization)



- Peak pressure – related to the breakage of the system.
- Final v – relevant to the performance of the system.

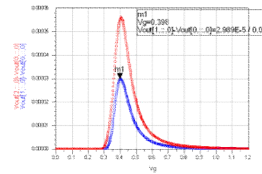
# THz Detector (UCSB Ph.D. 2003-2009)

$$\ddot{x} + \Gamma \dot{x} + \omega_p^2 x = -\frac{eE_{THz}}{m^*} e^{j\omega t}$$

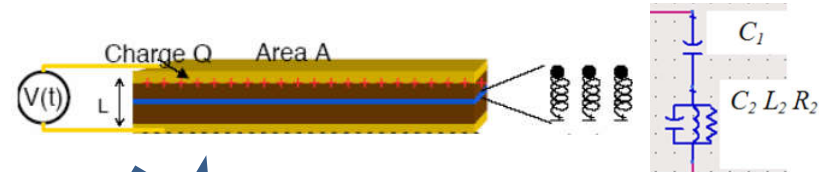
$$\Re_I = \frac{I_{signal}}{P_{in}} = \alpha \frac{e}{\epsilon \epsilon_0 \Gamma'} \text{Re}(\mu) \frac{dn}{dV_G} \quad (\text{A/W}).$$

$$NEP_I = \frac{\sqrt{4k_B T / R_{SD}}}{\Re_I} \quad (\text{W/Hz}^{1/2}).$$

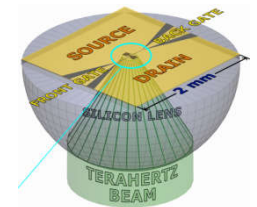
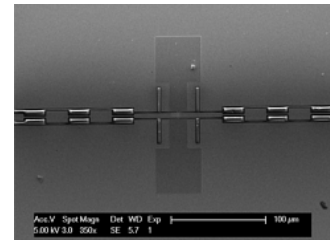
**Device  
Model  
Revision**



**Device  
Modeling**



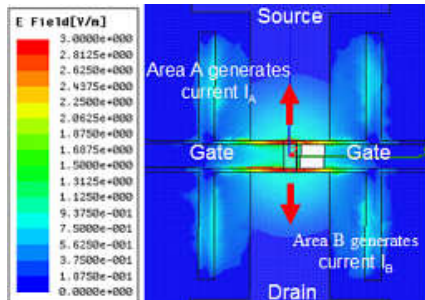
**Fabrication**



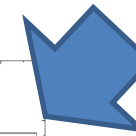
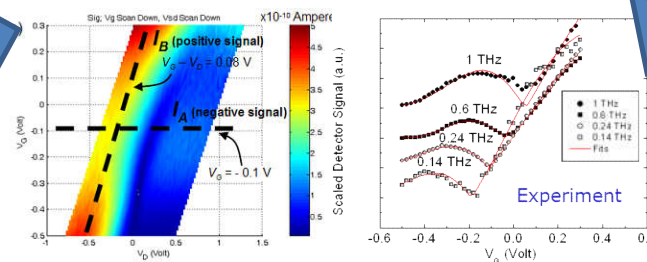
**Measurements**



**FEM EM  
Simulation**



**Data Analysis**

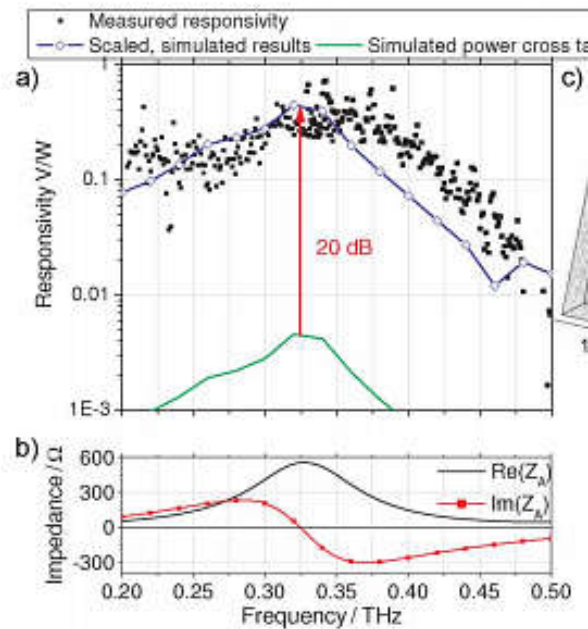


# THz Mixer (Tanner Research, 2009-2013)

**Device Modeling**

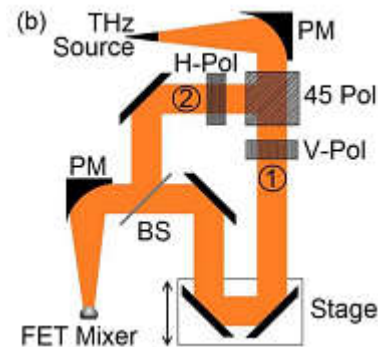
$$j_{SD} = n(\omega_G)ev(\omega_{SD})$$

$$U_r = \eta \left[ \frac{U_g^{\text{THz}} U_{\text{DS}}^{\text{THz}} \cos \varphi}{2(U_g^{\text{DC}} - U_{\text{DS}}^{\text{DC}})} - \frac{(U_{\text{DS}}^{\text{THz}})^2}{4(U_g^{\text{DC}} - U_{\text{DS}}^{\text{DC}})} \right]$$



**Data Analysis**

**Measurements**



**FEM EM Simulation**

**Cleanroom Fabrication**

**Thank you!**